Carbon Dioxide Capture Performance of Mesostructured Adsorbent Impregnated with Polyethylenimine

Chien-Hung Chen*, Ching-Tsung Yu, Yu-Fei Chang

Department of Chemistry, National Atomic Research Institute, Taoyuan, Taiwan, ROC

Received 22 January 2024; received in revised form 27 March 2024; accepted 28 March 2024

DOI: https://doi.org/10.46604/ijeti.2024.13298

Abstract

This study aims to investigate the CO_2 uptake performance of mesostructured adsorbents, such as Mobil Composition of Matter No. 41 (MCM-41), Santa Barbara Amorphous-15 (SBA-15), and multi-walled carbon nanotubes (MWNTs), modified with polyethylenimine (PEI). Mesoporous materials are loaded with 50 wt.% PEI using a wet impregnation method. CO_2 kinetic experiments of the PEI-modified adsorbents are conducted by a thermogravimetric method. The results reveal that the CO_2 adsorption capacities of the PEI/MCM-41, PEI/SBA-15, and PEI/MWNTs composites are 2.02, 3.06, and 2.93 mmol/g, respectively, under 15% CO_2 flow at 348 K. The lower CO_2 adsorption capacity of PEI/MCM-41 (2.02 mmol/g) is attributed to its poor porosity. The PEI/MWNTs composite has the fastest CO_2 adsorption and desorption kinetics at the same temperature, compared to other PEI-modified adsorbents. These results suggest that MWNTs might play a significant "separator" role in effectively dispersing the PEI molecular chains on the mesostructured adsorbent.

Keywords: polyethylenimine, CO_2 capture, kinetic model, mesoporous materials

1. Introduction

Reducing CO_2 emissions is widely recognized as a crucial goal in preventing the exacerbation of global climate change. The international energy agency (IEA) has highlighted that carbon capture, utilization, and storage (CCUS) will play a major role in achieving the target of "net zero by 2050" [1]. The economic feasibility and energy consumption of CO_2 capture technologies must be considered for the industrialization of CCUS. Amine scrubbing has been traditionally used for CO_2 capture for several decades. Amine solutions (e.g., methyldiethanolamine, diethanolamine, and monoethanolamine) have been employed for large-scale CO_2 capture under ambient conditions [2]. Unfortunately, amine scrubbing has significant disadvantages, including high energy consumption during amine regeneration, corrosion issues, and the management of degraded amine solutions [3].

The utilization of sorbents modified with organic amines has been explored as an effective adsorption technique for CO_2 capture. Xu et al. [4] proposed the "molecular basket" concept, involving the dispersion of an amine in a mesoporous material with a high surface area to enhance CO_2 capture through interaction with amino groups. Two feasible approaches, viz., impregnation [5] and grafting [6] have been examined to load amines onto/into mesoporous materials. Adsorbent preparation via impregnation is attractive because of its simplicity, low cost, and high amine loading. Potential amine candidates such as tetraethylenepentamine (TEPA) [7], polyethylenimine (PEI) [8], and ethylenediamine (EDA) [9] have undergone extensive investigation in numerous previous studies on CO_2 capture using a solid sorbent.

* Corresponding author. E-mail address: chchen1120@nari.org.tw

English language proofreader: Chih-Wen Teng

The results revealed that PEI exhibits more stable properties during cyclic CO_2 capture tests, compared to TEPA [9-10]. The porosity of the adsorbent also plays a crucial role in the CO_2 capture performance of amine-modified adsorbents. Aqueous amines can agglomerate and block the pore channel networks, leading to diffusion limitations and the deterioration of the CO_2 capture ability of the material.

As anticipated, mesostructured sorbents are more suitable for impregnation with amines than microstructured sorbents. Several sorbents, including Santa Barbara Amorphous-15 (SBA-15) [8], Matter No. 41 (MCM-41) [5], hexagonal mesoporous silica [11], and nanostructured carbon [12], have been proposed as potential supports for amines. It has been suggested that a high pore volume and large pore size of mesoporous materials are crucial factors for loading maximum amounts of amines with good dispersion.

Moreover, Heydari-Gorji et al. [13] reported that a high CO_2 capacity of 20.6 wt.% was obtained with pore-extend MCM-41 impregnated with 55 wt.% of PEI. This was attributed to the good dispersion of amine molecules in the large pores with a pore size of 11.4 nm (pore volume is 1.59 cm^3/g). Similar results have also been reported by others [14-15]. For the efficient use of a sorbent, ensuring suitable gas-solid contact significantly impacts the CO_2 capture efficiency and associated cost [16]. Various reactor configurations, including fixed beds, moving beds, and fluidized beds, have been discussed in previous reports [16-17]. Among these options, a fixed-bed reactor could be considered a favorable choice for CO_2 capture owing to its simple design. In addition to CO_2 capture, ensuring high-purity CO_2 recovery (> 90%) is a critical concern. Common purification and separation processes such as pressure swing adsorption [18], temperature swing adsorption [19], and vacuum swing adsorption (VSA) [20] have been developed.

As mentioned, the adsorption and desorption kinetics of CO_2 play a pivotal role in the practical applications of CO_2 capture and recovery systems. In this study, PEI was used as an amine to modify various mesostructured materials through impregnation. Subsequently, the CO_2 adsorption performance of the PEI-modified adsorbents was evaluated under 15 vol.% CO_2 flow (balanced with N_2) to simulate CO_2 capture from flue gas. To clarify the mechanism of CO_2 capture by the PEI-modified adsorbent, an investigation into the kinetics of CO_2 adsorption/desorption was conducted.

2. Experimental

(1) Preparation of adsorbent

Commercial PEI (Sigma-Aldrich, branched form, MW: approximately 800) was used to promote the CO_2 uptake ability of the adsorbents. Three mesostructured materials, viz., MCM-41(Sigma-Aldrich), SBA-15 (Sigma-Aldrich), and multi-walled carbon nanotubes (MWNTs; Conjutek Co., Ltd., diameter range: 15-25 nm) were selected as supports. PEI-modified sorbents were prepared using a wet impregnation method. Briefly, 500 mg of the sorbent powder was immersed in 20 mL of an ethanol solution of PEI, and the resulting mixture was stirred for 24 h under ambient conditions. During immersion, the PEI molecules are expected to disperse in the pore channels of MCM-41 and SBA-15, and on the external surface of the MWNTs. After the impregnation process, the mixtures were dried under vacuum using a rotary evaporator to remove the solvent. All the mixtures were subsequently dried at 333 K under a pressure of 10 mbar. The sorbents with 50 wt.% PEI loading are labeled as "PEI/MCM-41," "PEI/SBA-15," and "PEI/MWNTs," respectively.

(2) CO_2 adsorption/desorption tests

A thermogravimetric instrument (NETZSCH, STA 449 F3) was used to determine the CO_2 adsorption and desorption behaviors of the PEI-modified samples. All experiments were performed under a pressure condition of 0.1 MPa. Typically, approximately 10 mg of the sample was used in each analysis. Before the adsorption study, the sample was preheated at 373 K for 1 h with an N_2 flow of 30 mL/min to eliminate impurities. Subsequently, the samples were heated at 348 K under N_2

until the temperature was constant. Thereafter, 15 vol.% CO_2 (balanced by N_2) was introduced at 30 mL/min rate into the chamber, and the adsorption curves were collected. For desorption tests, the experiments were performed at 348 K under a N_2 flow of 30 mL/min, and the weight changes during desorption were recorded.

(3) Material characterization

N_2 adsorption/desorption isotherms were collected using a Micromeritics ASAP 2020 instrument. From the N_2 adsorption/desorption isotherms, the specific surface area was calculated using the Brunauer–Emmett–Teller (BET) equation. The total pore volume was calculated based on the amount of N_2 adsorbed at P/P_0 of 0.995.

3. Results and Discussion

In this study, the CO_2 uptake performances of different mesostructured adsorbents were investigated. The relationships between structural texture, CO_2 adsorption capacity, adsorption/desorption kinetics, and amine efficiency were examined to clarify the CO_2 capture mechanism of the PEI-modified adsorbent. The detailed results are outlined as follows.

3.1. Characterizations of adsorbents

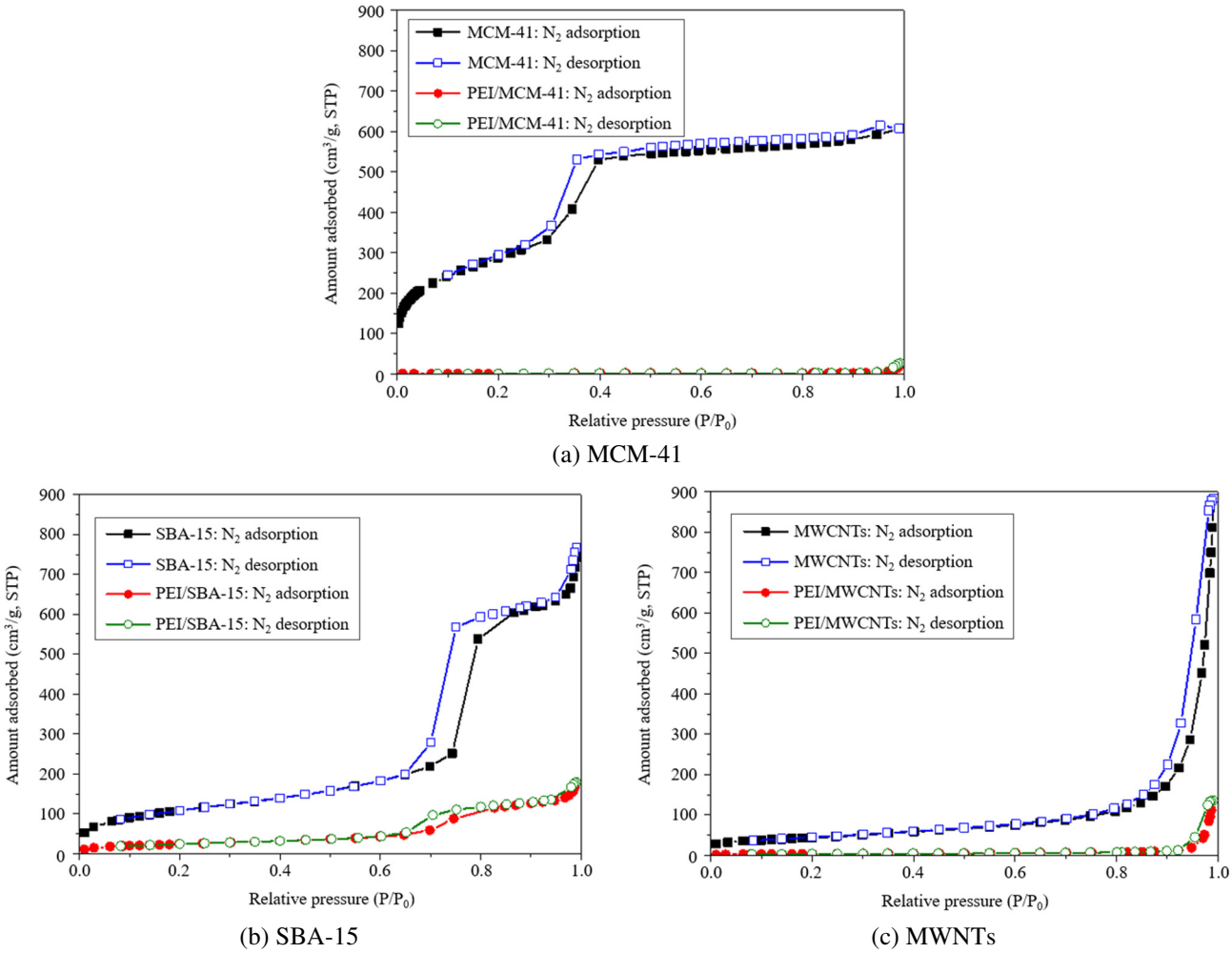

(a) MCM-41

(b) SBA-15

(c) MWNTs

Fig. 1 N_2 adsorption-desorption isotherm curves of different mesostructured adsorbents before and after PEI impregnation

In this study, three types of mesostructured adsorbents, viz., MCM-41, SBA-15, and MWNTs were used to support branched PEI, and then the CO_2 adsorption and desorption behaviors of the resulting composites were investigated. A PEI loading of 50 wt.% was used based on a previous study [5]. Fig. 1 presents the N_2 adsorption-desorption isotherms and Table 1 shows the extracted textural properties of various mesostructured materials before and after PEI impregnation. By the

International Union of Pure and Applied Chemistry (IUPAC) classification [21], the N_2 adsorption isotherms of the MCM-41, SBA-15, and MWNTs sorbents (before loading) were categorized as typical type IV with parallel H1 type hysteresis loops. These isotherms mainly indicate a mesoporous texture of the pristine adsorbent materials [6]. The hysteresis loops observed for different ranges of relative pressure suggest the presence of varied pore distributions in these adsorbent materials.

Table 1 Textural properties of mesostructured adsorbents

Samples	BET specific surface area (m^2/g)	V_t^{**} (cm^3/g)
MCM-41	948.0	0.933
PEI/MCM-41*	3.5	0.027
SBA-15	391.0	1.141
PEI/SBA-15*	88.7	0.271
MWNTs	156.9	1.280
PEI/MWNTs*	12.7	0.206

*: PEI loading was approximately 50 wt.%.
**: Total pore volume.

Both MCM-41 and SBA-15 with ordered mesoporous structures have been widely investigated in previous studies [5-6]. Materials with large pore volumes and pore sizes allow a higher loading of amino group-containing polymers and facilitate CO_2 diffusion. MCM-41 and SBA-15 were determined to have large pore volumes of 0.933 and 1.141 cm^3/g, respectively, consistent with previously reported results [9, 17]. The MWNTs also had a larger pore volume of 1.280 cm^3/g, possibly attributed to inter-MWNTs and/or intra-MWNTs spaces [22].

After the loading of 50 wt.% PEI, the N_2 adsorption–desorption isotherms of the composites changed significantly, indicating a decrease in the porosity of the mesostructured sorbents after PEI impregnation. This phenomenon can be attributed to the dispersion of PEI molecules within the mesoporous structure, forming “molecular baskets” [4]. For PEI/MCM-41, the mesoporous characteristic was not found, as shown in Fig. 1(a). The specific surface area and total pore volume of PEI/MCM-41 were calculated to be 3.5 and 0.027 cm^3/g, respectively, indicating a significant reduction in the porosity of MCM-41 after the impregnation of 50 wt.% PEI.

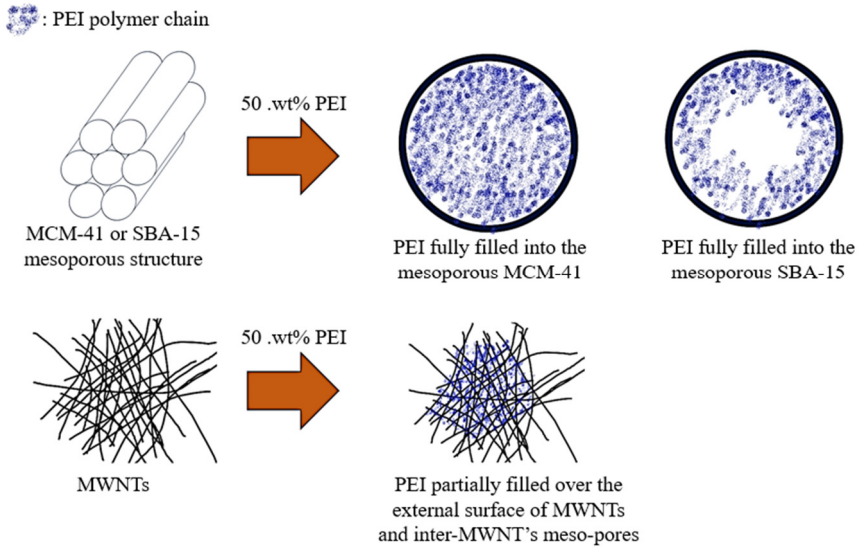

Fig. 2 Schematic of the status of PEI in mesostructured adsorbents

In contrast, the N_2 adsorption-desorption isotherm of PEI/SBA-15 retained the type IV characteristic with a parallel H1-type hysteresis loop. Considering the density of PEI at approximately 1 g/mL, the theoretical maximum amounts of PEI loaded into MCM-41 and SBA-15 are 47 and 57 wt.%, respectively. In this study, the actual amount of PEI loaded (54.1 wt.%) into MCM-41 slightly exceeded the theoretical value of 47 wt.%. According to N_2 adsorption analysis, the pore volume of the MCM-41 sample decreased significantly from 0.933 to 0.027 cm^3/g after PEI loading. This result indicates that PEI not only

filled the mesopores in MCM-41 but also dispersed on the external surface of the MCM-41 particles. In contrast, PEI was not fully dispersed in the nanochannels of SBA-15. The remaining porous space benefits CO_2 diffusion during the adsorption and desorption processes.

In the case of PEI/MWNTs, the PEI molecule is expected to have difficulty diffusing into the interior of the MWNTs due to mass transfer resistance. In this study, the MWNTs act as separators to disperse the PEI molecules on their external surfaces and in the inter-MWNTs pores. After PEI loading, the inter-MWNTs porosity decreased from 1.280 to 0.206 cm^3/g. Fig. 2 presents a schematic of the structures of the PEI/MCM-41, PEI/SBA-15, and PEI/MWNTs composites based on their porosity. In this work, the PEI-loading status of PEI/MCM-41, PEI/SBA-15, and PEI/MWNTs is assumed to be "fully filled in mesopores," "partially filled in mesopores," and "partially filled over the external surface," respectively.

3.2. CO_2 capture performance

In this study, CO_2 adsorption tests were conducted on the PEI-modified adsorbents at 348 K under 15% CO_2 atmosphere. The CO_2 adsorption capacities of the PEI-modified adsorbents and the amine efficiency in capturing CO_2 (mmol CO_2/mmol N) are listed in Table 2. Despite a similar PEI loading, the CO_2 adsorption capacity of PEI/MCM-41 (2.02 mmol/g) was lower than those of the other two. A lower amine efficiency was also observed for PEI/MCM-41, which can be attributed to poor porosity and significant resistance to mass transfer in PEI/MCM-41. The amine efficiency of CO_2 capture in the PEI-impregnated sorbents ranged from 0.2 to 0.3, strongly depending on the sorbent's porosity and the dispersion status of PEI [8, 17].

Table 2 CO_2 adsorption performance of PEI-impregnated adsorbents

	T (K)	CO_2 (%)	CO_2 adsorption capacity (mmol-CO_2/g)	Amine loading (mmol-N/g)*	Amine efficiency (mmol CO_2/mmol N)
PEI/MCM-41	348	15	2.02	12.6	0.16
PEI/SBA-15	348	15	3.06	11.6	0.26
PEI/MWNTs	348	15	2.93	11.1	0.26

*: Actual amine loading was determined by thermal decomposition

In this study, both PEI/SBA-15 and PEI/MWNTs exhibited a good amine efficiency of 0.26. Similar results have been reported in previous studies [5]. The remaining porosity of the adsorbent after PEI loading plays a crucial role in facilitating the mass transfer of CO_2. To clarify the related mechanism, the kinetics of CO_2 capture by the PEI-modified mesostructured materials were investigated.

3.3. Adsorption kinetics

Pseudo-first-order and pseudo-second-order models are widely used to describe the adsorption kinetics of gases [23]. The pseudo-first-order model is given by

$$\frac{dq}{dt} = k_1 \left(q_e - q_t \right) \tag{1}$$

where q_e is the adsorbed equilibrium capacity, q_t is the adsorbed capacity and a function of time, and k_1 is the first-order kinetic constant. After integration of Eq. (1) with the boundary condition of $t = 0$, $q_t = 0$, and t = infinite, $q_t = q_e$, the pseudo-first-order model can be written as

$$q_t = q_e \left(1 - e^{-k_1 t} \right) \tag{2}$$

The linear relationship between $(q_e - q_t)$ and t, can be expressed as

$$\ln \left(q_t - q_e \right) = \ln \left(q_e - k_1 t \right) \tag{3}$$

In addition, the pseudo-second-order model [23] is given by

$$\frac{dq}{dt} = k_2 \left(q_e - q_t\right)^2 \tag{4}$$

where k_2 is the second-order kinetic constant. With the boundary conditions of $t = 0$, $q_t = 0$, and t = infinite, $q_t = q_e$, the pseudo-second-order model can be written as

$$q_t = \frac{q_e^2 k_2 t}{1 + q_e k_2 t} \tag{5}$$

The linear relationship between $(q_e - q_t)$ and t, can be expressed as

$$\frac{t}{q_t} = \frac{1}{k_2 q_e^2} + \frac{1}{q_e} t \tag{6}$$

To determine the adequacy of each model, the normalized standard deviation (an error function, Err) is calculated as follows:

$$Err(\%) = \sqrt{\frac{\left[\left(q_{t(\exp)} - q_{t(\text{model})}\right)/q_{t(\exp)}\right]^2}{N-1}} \tag{7}$$

Fig. 3 shows the experimental CO_2 uptake curves for the PEI-modified adsorbents. As illustrated in Fig. 3(a), both the CO_2 adsorption capacity and adsorption rate of the samples increased with increasing temperature. According to previous studies [5, 17], the optimal temperature for CO_2 uptake by PEI-impregnated material systems is 348 K. The reaction of CO_2 with the amino group is an exothermic reaction with an adsorption heat of −50 to −60 kJ/mol [24]. PEI is a viscous polymer, and its reactivity is expected to be low at lower temperatures (e.g., room temperature). As the temperature increases from room temperature to 348 K, PEI becomes more flexible, facilitating the diffusion of CO_2 molecules. Indeed, optimal CO_2 adsorption by the PEI-modified material is governed by dynamics rather than thermodynamics [25].

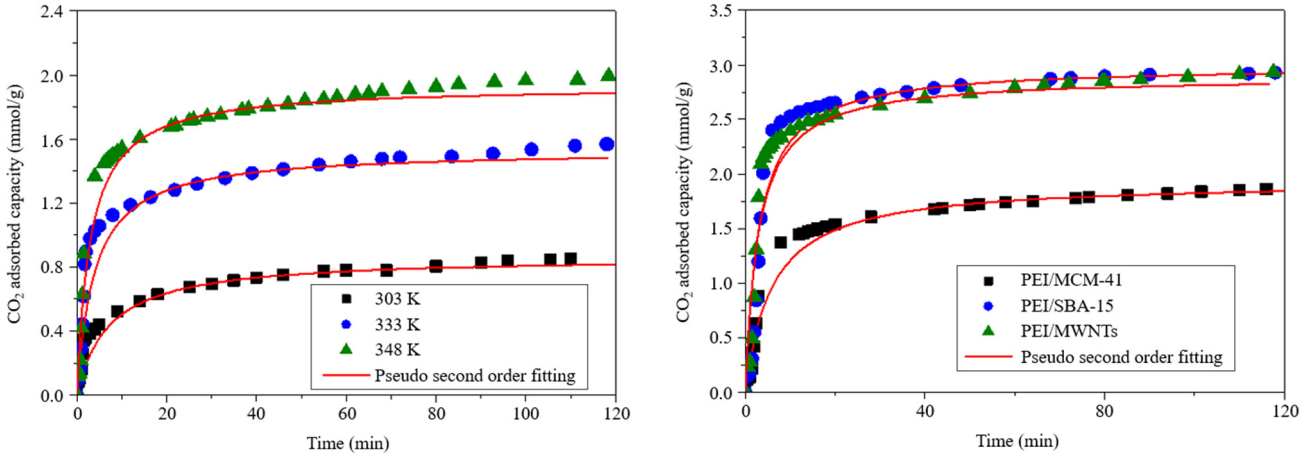

(a) CO_2 adsorption on PEI/MCM-41 at different temperatures (b) CO_2 adsorption on different PEI modified adsorbents at 348 K

Fig. 3 Experimental CO_2 uptake curves for the PEI-modified adsorbents

In this study, pseudo-first-order and pseudo-second-order models were used to fit the adsorption kinetic data of PEI-modified adsorbents, and the fitting parameters are listed in Table 3. The results indicate that the experimental data of CO_2 adsorption by PEI-modified adsorbents can be better fitted with the pseudo-second-order kinetic model. The Err values of approximately 10% for pseudo-second-order fitting are significantly lower than those for pseudo-first-order fitting. The fitting parameters reveal that the kinetic constant k_2 increases with increasing temperature, which is consistent with a previous report [24]. Additionally, the k_2 values of the PEI-modified samples can be ranked as follows: PEI/MWNTs > PEI/SBA-15 > PEI/MCM-41.

Table 3 Values of the CO_2 adsorption kinetic model parameters

Sample	T (°C)	$q_{e,exp}$ (mmol/g)	Pseudo-first-order			Pseudo-second-order		
			$q_{e,cal}$ (mmol/g)	k_1 (1/min)	Err (%)	$q_{e,cal}$ (mmol/g)	k_2 (g/mmol min)	Err (%)
PEI/MCM-41	30	1.25	0.75	0.009	69	0.86	0.161	10.4
	60	1.56	0.53	0.026	75	1.53	0.166	7.6
	75	2.02	0.59	0.023	79	1.93	0.172	8.1
PEI/SBA-15	75	3.06	0.48	0.024	89	3.00	0.219	10.8
PEI/MWNTs	75	2.93	0.73	0.053	88	2.89	0.238	7.0

This result implies that the mass transfer resistance of CO_2 adsorption by PEI/MCM-41 is expected to be lower than those of the other two PEI-modified samples. Several studies [23-24, 26] have reported CO_2 capture kinetics for amine-modified adsorbents. Al-Marri et al. [26] used a double-exponential model to fit the data of CO_2 adsorption to branched PEI-impregnated mesoporous silica. Bai et al. [24] employed the Avrami kinetic model to fit the data of CO_2 uptake by a PEI-impregnated resin (HPD450) in the temperature range of 298 to 363 K. The exponent of the kinetic equation (n) was in the range of 0.342 to 0.757. Liu et al. [23] also indicated that the CO_2 adsorption curve of TEPA-impregnated MWNTs could be fitted well with the Avrami kinetic model, and the exponent of the equation ranged from 1.1 to 1.6.

3.4. Desorption kinetics

Avrami's model was favorable to fit the CO_2 desorption of PEI-modified sorbent [23], and it can be expressed as:

$$\alpha = 1 - \frac{q_t}{q_e} = 1 - \exp\left[-k_A (t)^n\right] \tag{8}$$

where α represents the desorption ratio, k_A is the desorption rate constant and n is the exponent of Avrami's equation. The linearized form of Eq. (8) can be expressed as:

$$\ln\left[-\ln(1-\alpha)\right] = n \ln k_A + n \ln t \tag{9}$$

Fig. 4 shows the desorption kinetic curves for different PEI-modified adsorbents. The CO_2 desorption rate of PEI/MWNT was higher than that of the other samples. Similar results were obtained for the adsorption process at the same operating temperature (e.g., 348 K). This result indicates that the CO_2 diffusion resistance of PEI/MWNT is lower than those of the other samples. This is because the textural porosity of MCM-41 fully filled with PEI molecules is unfavorable for CO_2 adsorption and desorption. Thus, the mass transfer resistance strongly affected CO_2 adsorption-desorption by the PEI-modified solid adsorbents.

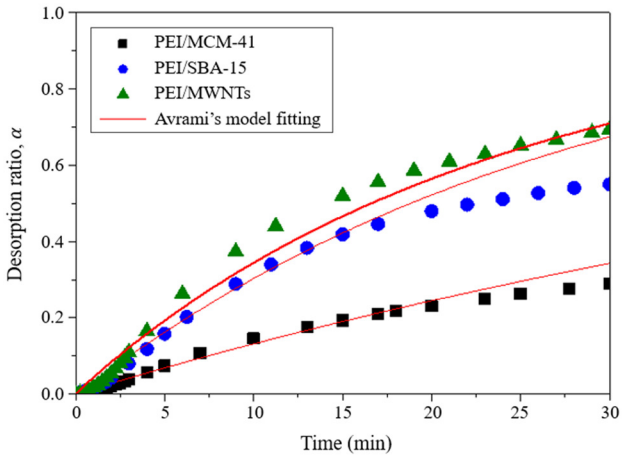

Fig. 4 Desorption proportion of PEI-modified adsorbents at 348 K

The CO_2 desorption kinetic fitting parameters obtained using the Avrami model are listed in Table 4. The k_A values are ranked as follows: PEI/MCM-41 < PEI/SBA-15 < PEI/MWNT. The exponent of the Avrami kinetic model was calculated to be in the range of 0.97 to 1.03. A similar fitting result was obtained by Al-Marri et al. [26], who reported that the CO_2 desorption curve for PEI-impregnated mesoporous silica followed first-order kinetics.

Table 4 Values of the CO_2 desorption kinetic model parameters

	Avrami's model fitting parameters		
Sample	k_A	n	Err (%)
PEI/MCM-41	0.0143	0.993	10.9
PEI/SBA-15	0.0335	1.032	13.7
PEI/MWNTs	0.0442	0.979	9.2

3.5. *Intraparticle diffusion model*

To understand the CO_2 adsorption mechanism, the simplest approximation of the intraparticle diffusion kinetics [27] was employed to identify the adsorption mechanism and predict the rate-controlling step. This relationship can be expressed as follows:

$$q_t = k_{id} t^{1/2} + C \tag{10}$$

where k_{id} (mmol g^{-1} $min^{0.5}$) is the intraparticle diffusion rate constant. C is the intercept.

Fig. 5 shows the intraparticle diffusion plots, that is, adsorption capacity q_t vs. the square root of time t for the PEI-loaded adsorbents. According to this model, if intraparticle diffusion is the sole rate-controlling step, the plot is linear and passes through the origin [27]. Three linear regions were observed for all the PEI-modified samples. The three linear portions labeled as regions I, II, and III represent external mass transfer (film diffusion), gradual adsorption, and final equilibrium stage, respectively.

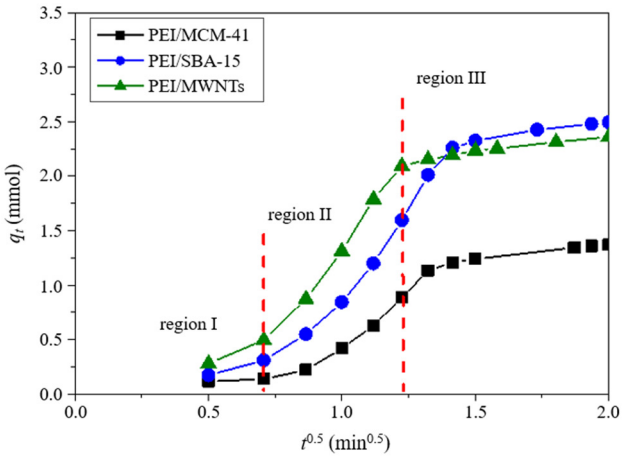

Fig. 5 Intraparticle diffusion plots of adsorption capacity q_t vs. the square root of time t

As shown in Fig. 5, the plot of q_t against t 0.5 for all regions reveals that the straight lines do not pass through the origin, implying that intraparticle diffusion is not the rate-controlling step for CO_2 adsorption to the PEI-modified adsorbent systems. It is noted that intraparticle diffusion became insignificant when the mesoporous adsorbent was loaded with a high amount of PEI.

3.6. *Boyd's film-diffusion model*

In addition, Boyd's film-diffusion model [27] was also employed to determine the actual rate-controlling step and can be expressed as:

$$F = \frac{q_t}{q_e} = 1 - \frac{6}{\pi^2}\sum_{n=1}^{\infty}\frac{1}{n^2}\exp\left(-n^2 B_t\right) \tag{11}$$

where F is the fractional adsorption capacity. B_t is a function of F.

For $F < 0.85$, The relationship between B_t and F can be expressed as:

$$B_t = \left(\sqrt{\pi} - \sqrt{\pi - \frac{\pi^2 F}{3}}\right)^2 \tag{12}$$

For $F > 0.85$, The relationship between B_t and F can be expressed as:

$$B_t = -0.4977 - \ln\left(1 - F\right) \tag{13}$$

A plot of B_t versus time (min) was used to distinguish between film diffusion (external transport) and intraparticle diffusion. If the plot is straight and passes through the origin, the adsorption rate is governed by intraparticle diffusion [27]. Otherwise, the kinetics is governed by film diffusion, which is the rate-controlling step. Fig. 6 shows the plots of B_t value vs. time for the different PEI-modified adsorbents. A linear plot that does not pass through the origin is found for the PEI/MCM-41 sample. On the other hand, the Boyd plot is neither linear nor passes through the origin for PEI/SBA-15 and PEI/MWNT. According to Boyd's assumptions [28], film diffusion (external transport) governs the adsorption kinetics for CO_2 uptake by PEI-modified nanostructured adsorbents. The results were confirmed by intraparticle diffusion model analysis (as shown in Fig. 5).

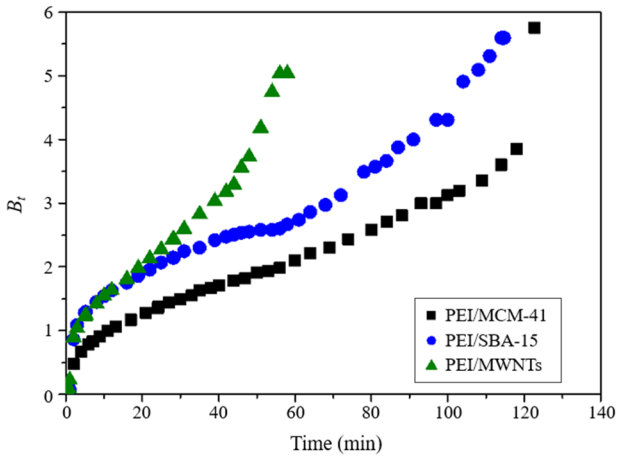

Fig. 6 Plots of B_t value vs. time for PEI-modified adsorbents

4. Conclusion

In this study, the CO_2 adsorption/desorption kinetics of mesostructured adsorbents loaded with 50 wt.% PEI was investigated. The CO_2 capture performance was evaluated with 15% CO_2 flow (balanced by N_2) in the temperature range of 303 to 348 K. The experiments revealed that the CO_2 adsorption performance was significantly dominated by the dynamics due to the mass transfer resistance. In the kinetic studies, the porosity of the PEI-modified adsorbent strongly affected the adsorption and desorption rates. Based on the favorable adsorption/desorption kinetics of the PEI/MWNTs adsorbent, they are more advantageous for industrial applications in vacuum swing adsorption (VSA) processes for carbon dioxide capture and separation compared to other samples (PEI/MCM-41 and PEI/SBA-15).

Acknowledgments

The work was supported by the National Science and Technology Council, Taiwan, ROC (NSTC 112-2218-E-042A-001).

Conflicts of Interest

The authors declare no conflict of interest.

References

[1] International Energy Agency, "Net Zero by 2050: A Roadmap for the Global Energy Sector," IEA, Special Report, 2021.

[2] M. Waseem, M. Al-Marzouqi, and N. Ghasem, "A Review of Catalytically Enhanced CO2-Rich Amine Solutions Regeneration," Journal of Environmental Chemical Engineering, vol. 11, no. 4, article no. 110188, August 2023.

[3] R. Neerup, V. E. Rasmussen, S. H. B. Vinjarapu, A. H. Larsen, M. Shi, C. Andersen, et al., "Solvent Degradation and Emissions from a CO2 Capture Pilot at a Waste-to-Energy Plant," Journal of Environmental Chemical Engineering, vol. 11, no. 6, article no. 111411, December 2023.

[4] X. Xu, C. Song, J. M. Andresen, B. G. Miller, and A. W. Scaroni, "Novel Polyethylenimine-Modified Mesoporous Molecular Sieve of MCM-41 Type as High-Capacity Adsorbent for CO2 Capture," Energy & Fuels, vol. 16, no. 6, pp. 1463-1469, November 2002.

[5] D. Panda, V. Kulkarni, and S. K. Singh, "Evaluation of Amine-Based Solid Adsorbents for Direct Air Capture: A Critical Review," Reaction Chemistry & Engineering, vol. 8, no. 1, pp. 10-40, January 2023.

[6] K. S. K. Reddy, A. M. Varghese, A. E. Ogungbenro, and G. N. Karanikolos, "Aminosilane-Modified Ordered Hierarchical Nanostructured Silica for Highly-Selective Carbon Dioxide Capture at Low Pressure," ACS Applied Engineering Materials, vol. 1, no. 2, pp. 720-733, February 2023.

[7] V. O. Viola, T. F. de Aquino, S. T. Estevam, B. Bonetti, H. G. Riella, C. Soares, et al., "Synthesis and Application of Two Types of Amine Sorbents Impregnated on Silica from Coal Fly Ash for CO2 Capture," Results in Engineering, vol. 20, article no. 101596, December 2023.

[8] M. Yang, S. Wang, and L. Xu, "Hydrophobic Functionalized Amine-Impregnated Resin for CO2 Capture in Humid Air," Separation and Purification Technology, vol. 315, article no. 123606, June 2023.

[9] B. Dziejarski, J. Serafin, K. Andersson, and R. Krzyżyńska, "CO2 Capture Materials: A Review of Current Trends and Future Challenges," Materials Today Sustainability, vol. 24, article no. 100483, December 2023.

[10] X. Xu, M. B. Myers, F. G. Versteeg, B. Pejcic, C. Heath, and C. D. Wood, "Direct Air Capture (DAC) of CO2 Using Polyethylenimine (PEI) "Snow": A Scalable Strategy," Chemical Communications, vol. 56, no. 52, pp. 7151-7154, July 2020.

[11] T. V. R. Mohan, P. Sridhar, and P. Selvam, "Experimental and Modelling Studies of Carbon Dioxide Capture onto Pristine, Nitrogen-Doped, and Activated Ordered Mesoporous Carbons," RSC Advances, vol. 13, no. 2, pp. 973-989, 2023.

[12] H. Li, "CO2 Capture by Various Nanoparticles: Recent Development and Prospective," Journal of Cleaner Production, vol. 414, article no. 137679, August 2023.

[13] A. Heydari-Gorji, Y. Yang, and A. Sayari, "Effect of the Pore Length on CO2 Adsorption over Amine-Modified Mesoporous Silicas," Energy & Fuels, vol. 25, no. 9, pp. 4206-4210, September 2011.

[14] S. Loganathan, M. Tikmani, A. Mishra, and A. K. Ghoshal, "Amine Tethered Pore-Expanded MCM-41 for CO2 Capture: Experimental, Isotherm and Kinetic Modeling Studies," Chemical Engineering Journal, vol. 303, pp. 89-99, November 2016.

[15] S. Loganathan and A. K. Ghoshal, "Amine Tethered Pore-Expanded MCM-41: A Promising Adsorbent for CO2 Capture," Chemical Engineering Journal, vol. 308, pp. 827-839, January 2017.

[16] C. Dhoke, A. Zaabout, S. Cloete, and S. Amini, "Review on Reactor Configurations for Adsorption-Based CO2 Capture," Industrial & Engineering Chemistry Research, vol. 60, no. 10, pp. 3779-3798, March 2021.

[17] F. Raganati, F. Miccio, and P. Ammendola, "Adsorption of Carbon Dioxide for Post-Combustion Capture: A Review," Energy & Fuels, vol. 35, no. 16, pp. 12845-12868, August 2021.

[18] H. Lin, J. Lu, A. M. Abed, K. Nag, M. Fayed, A. Deifalla, et al., "Simulation of CO2 Capture from Natural Gas by Cyclic Pressure Swing Adsorption Process Using Activated Carbon," Chemosphere, vol. 329, article no. 138583, July 2023.

[19] A. S. Akdag, I. Durán, G. Gullu, and C. Pevida, "Performance of TSA and VSA Post-Combustion CO2 Capture Processes with a Biomass Waste-Based Adsorbent," Journal of Environmental Chemical Engineering, vol. 10, no. 6, article no. 108759, December 2022.

[20] Z. Wang, L. Liu, G. Tian, T. Ren, Z. Qi, and G. K. Li, "Effect of Isopropanol on CO2 Capture by Activated Carbon: Adsorption Performance and Regeneration Capacity," Chemical Engineering Research and Design, vol. 196, pp. 632-641, August 2023.

[21] M. Thommes, K. Kaneko, A. V. Neimark, J. P. Olivier, F. Rodriguez-Reinoso, J. Rouquerol, et al., "Physisorption of Gases, with Special Reference to the Evaluation of Surface Area and Pore Size Distribution (IUPAC Technical Report)," Pure and Applied Chemistry, vol. 87, no. 9-10, pp. 1051-1069, October 2015.

[22] H. Hu, T. Zhang, S. Yuan, and S. Tang, "Functionalization of Multi-Walled Carbon Nanotubes with Phenylenediamine for Enhanced CO2 Adsorption," Adsorption, vol. 23, no. 1, pp. 73-85, January 2017.

[23] Q. Liu, J. Shi, S. Zheng, M. Tao, Y. He, and Y. Shi, "Kinetics Studies of CO2 Adsorption/Desorption on Amine-Functionalized Multiwalled Carbon Nanotubes," Industrial & Engineering Chemistry Research, vol. 53, no. 29, pp. 11677-11683, July 2014.

[24] G. Bai, Y. Han, P. Du, Z. Fei, X. Chen, Z. Zhang, et al., "Polyethylenimine (PEI)-Impregnated Resin Adsorbent with High Efficiency and Capacity for CO2 Capture from Flue Gas," New Journal of Chemistry, vol. 43, no. 46, pp. 18345-18354, December 2019.

[25] X. Wang, L. Chen, and Q. Guo, "Development of Hybrid Amine-Functionalized MCM-41 Sorbents for CO2 Capture," Chemical Engineering Journal, vol. 260, pp. 573-581, January 2015.

[26] M. J. Al-Marri, Y. O. Kuti, M. Khraisheh, A. Kumar, and M. M. Khader, " Kinetics of CO2 Adsorption/Desorption of Polyethyleneimine-Mesoporous Silica," Chemical Engineering & Technology, vol. 40, no. 10, pp. 1802-1809, October 2017.

[27] Y. Teng, Z. Liu, G. Xu, and K. Zhang, "Desorption Kinetics and Mechanisms of CO2 on Amine-Based Mesoporous Silica Materials," Energies, vol. 10, no. 1, article no. 115, January 2017.

[28] K. O. Yoro, M. K. Amosa, P. T. Sekoai, J. Mulopo, and M. O. Daramola, "Diffusion Mechanism and Effect of Mass Transfer Limitation during the Adsorption of CO2 by Polyaspartamide in a Packed-Bed Unit," International Journal of Sustainable Engineering, vol. 13, no. 1, pp. 54-67, 2020.